

Generation of Spherical and Monodisperse Particles of Poly(styrene) and Poly(methyl methacrylate) by Atomization of Monomers and Dissolved Polymer Precursors

THOMAI PANAGIOTOU and YIANNIS A. LEVENDIS*

Department of Mechanical Engineering, Northeastern University, Boston, Massachusetts 02115

SYNOPSIS

A technique to produce spherical and monodisperse particles of selected polymers is presented. Liquid precursors of either mixtures of organic monomers and initiator catalysts or polymers dissolved in organic solvents were sprayed inside a vertical thermal reactor. The temperature range in the reactor was 400–670 K and the experiments were conducted in a nitrogen atmosphere. Atomization was achieved by an acoustically excited aerosol generator. Batches of equal size particles of two thermoplastic materials, poly(styrene) and poly(methyl methacrylate), were obtained in the range of 30–60 μm in diameter. Elemental analysis showed that the C and H composition of the produced particles was very close to theoretically expected values. The thermal environment, atomization conditions, and residence times the particles experienced in the reactor were explored using numerical techniques; residence times in the order of 4–10 s were estimated.

INTRODUCTION

Production of small, homogeneous polymer particles of controlled size are of technological interest to the plastics, catalyst, and others industries.¹ Moreover, if the particles are produced spherical and monodispersed they can find further applications in fundamental studies of material properties, calibration of instruments, etc. Commonly, monodispersed particles have been produced from polymer colloids by emulsion or suspension polymerization. Everett and coworkers^{2,3} discussed the preparation of near spherical, 100 μm , poly(vinyl chloride) (PVC), poly(vinylidene chloride) (PVDC), and submicron poly(acrylonitrile) powders from dispersion polymerization. A similar technique was followed by Pendleton et al.⁴ to produce submicron (0.1 μm) PVDC particles. Howard and Knutton⁵ prepared large spherical carbon particles ($\approx 500 \mu\text{m}$) from the thermal degradation of crosslinked polymeric

beads, made from the suspension polymerization of mixtures of PVDC and ethylene dimethylacrylate. These materials yielded porous beads upon carbonization.

Bhanti et al.⁶ generated poly(styrene) particles by nebulizing a polymer solution in xylene and evaporating the solvent. Subsequent size classification and second-stage atomization after resuspending the colloids in water was necessary to produce a monosized aerosol. Matijević and coworkers⁷ produced fairly uniform, micron size poly(urea) particles by reacting liquid aerosol droplets of toluene diisocyanate with ethylenediamine vapor. The same aerosol technique was used for polymerization of styrene monomer droplets in vapors of the initiator trifluoromethanesulfonic acid (TFSA).⁸ The above investigators also produced (8 μm) poly(divinylbenzene) particles using the same aerosol technique.⁹ These particles shrank to porous 3–5 μm spheroid residues upon carbonization at 500°C.¹⁰

An alternative technique was used by Levendis and Flagan^{11,12} to produce monodisperse solid carbon particles (5–200 μm) to be used in combustion stud-

* To whom correspondence should be addressed.

ies. The method utilized an aerosol generator to atomize various mixtures of poly(furfuryl alcohol) and pore-forming agents dissolved in acetone. The mixtures were sprayed inside a thermal reactor where secondary polymerization (curing) took place. The work described herein pertains to the production of poly(styrene) and poly(methyl methacrylate) particles using the above technique, to either atomize solutions of these two polymers in solvents, or atomize and polymerize their liquid monomer precursors. In both cases, solid polymer particles were formed in the thermal reactor. In the latter case, the polymerization was conducted and completed inside the reactor. In this manner, the rate of polymerization of the two thermoplastics was expedited and plastic powders were produced in a matter of seconds.

EXPERIMENTAL

Aerosol Generator

To produce spherical and monodisperse drops from a polymeric fluid, an aerosol generator was constructed based on the design of Levendis and Flagan,¹² shown in Figure 1. In this instrument, a continuous flow of liquid is forced through a small orifice. Concurrently, the liquid in the generator's cavity is oscillated at a high frequency using a piezoelectric transducer. The vibration creates an instability that leads to the break-up of the liquid jet into uniformly sized droplets. The size of the droplets is controlled by the size of the orifice, the oscillator frequency, and the liquid feed rate. Consequently, the size of the dried particle depends on all of the above parameters in addition to the degree of dilution of the polymer (mass fraction of solvent). In the present experiments, to produce particles of sizes in the range of 30–60 μm , monomers or polymers under various degrees of dilution were used in

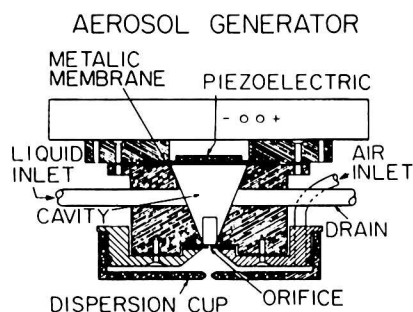


Figure 1 Schematic of the acoustically excited aerosol generator.

conjunction with 75- μm orifices, frequencies of 16–18 kHz, and a flowrate of 1.6 cc/min. The piezoelectric elements used were silver electrode bimorphs (Vernitron PZT5H and Piezo Kinetics PZT-550) 1.25 cm in diameter and 0.62 mm thick. They were glued with a conductive silver epoxy (Tra-Con) on thin stainless steel metallic membranes 25–75 μm (thickness). These transducers were driven by a function generator at 20 V amplitude.

The pinholes were laser drilled for precision (Melles Griot). A high-pressure syringe pump (Harvard Apparatus 909) was used to feed liquid polymers to the generator via (Becton Dickinson) plastic syringes.

Thermal Reactor

A thermal reactor was constructed for the drying and curing of the droplets that were generated at the top of the reactor, where the aerosol generator was mounted (Fig. 2). This stainless steel flow reactor is 1.5 m high, 0.1 m i.d., and is externally heated in two stages by cylindrical (Thermocraft) heating elements. They are controlled by separate (Omega) temperature controllers and supply 3,800 W at the top and 3,000 W at the bottom sections, providing wall temperatures up to 1,000 K. The aerosol generator is placed at the top of the reactor on a special flange that incorporates provisions for introduction of dilution gas (nitrogen). This gas passes through a flow straightener and flows downward engulfing the stream of droplets. A secondary stream of gas flows through a small orifice concentric with the aerosol jet (Figs. 1 and 2) to disperse the droplets and prevent coagulation.

A quartz observation window is mounted on the top to facilitate monitoring of the operation and uniformity of the jet. To check for monodispersivity of the droplets, provisions for a small gas jet to impinge perpendicularly to the droplet stream have been made. In this manner, droplets of equal size deflect at the same angle; meanwhile, polydisperse droplets deflect at a multitude of angles (satellites). Monodispersion can be accomplished by adjusting the flowrate and finely tuning the frequency. Theoretically, the frequency range for monodispersivity is $1/7D_j < f < 1/3.5D_j$, where D_j is the orifice diameter.¹³ Directly below the observation window an orifice plate has been inserted to improve the flow conditions, as discussed in a following section. At the bottom of the reactor a virtual impactor stage has been constructed to aid in the collection of dry particles and eliminate small micron-size particles formed by various mechanisms, such as condensa-

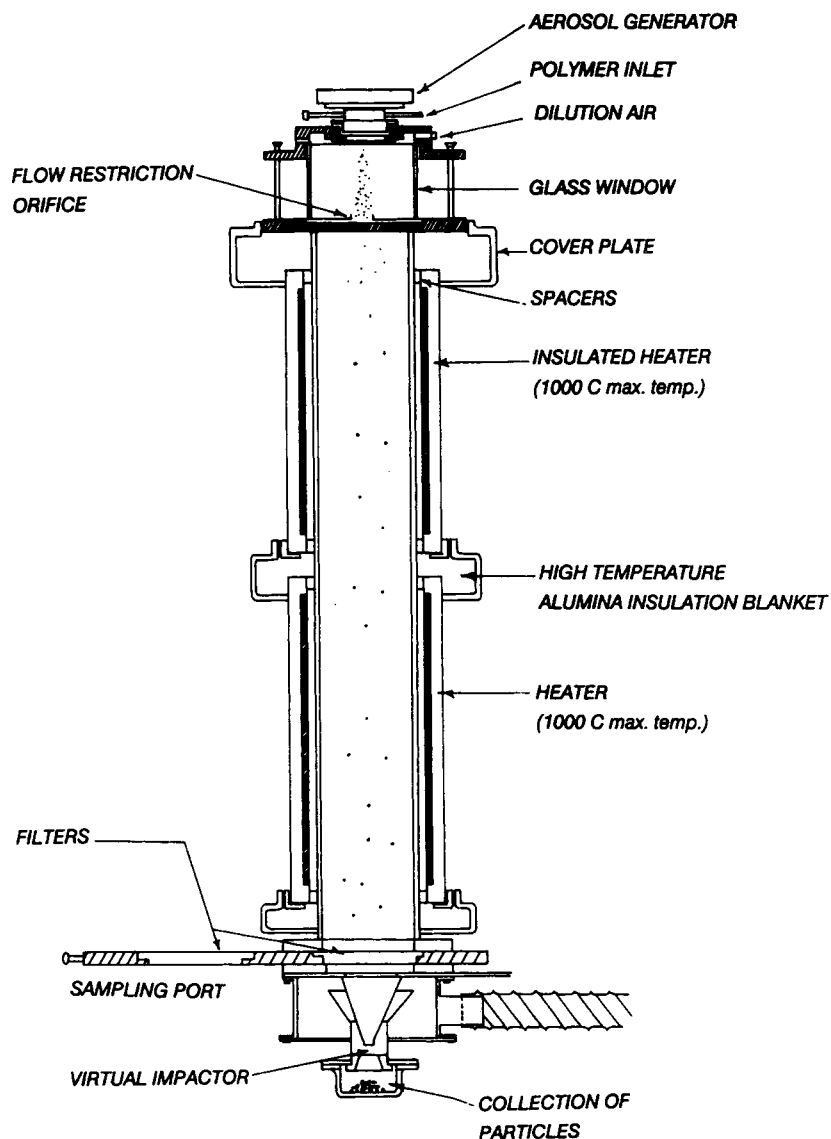


Figure 2 Two stage thermal reactor.

tion of vapors. A sampling filter stage has also been incorporated.

PRODUCTION OF POLYMERS

To produce the polymers required for this study, two different techniques were employed: (1) aerosol production of dissolved polymers with subsequent evaporation of the solvent in the reactor and (2) aerosol production of partially polymerized precursors in a solvent with subsequent evaporation of the solvent and sequential completion of the polymerization in the reactor. Both techniques can also be applicable to any other polymers that can be com-

pletely dissolved in solvents and to monomers whose polymerization can be achieved in bulk and is readily controlled.

Poly(styrene)

Polystyrene particles were produced with both of the above techniques.

1. An aerosol of commercially available polystyrene (Styron 685-D, Dow Chemical) dissolved in toluene was generated. Solutions of 2.5 wt % polystyrene in toluene were used in conjunction with a 75- μm orifice, a flowrate of 1.6 cc/min, and an excitation frequency of

17 kHz. The gas (nitrogen) flowrates in the reactor were ≈ 1 lpm dispersion and 2.5 lpm dilution. The maximum wall temperature at the upper section of the thermal reactor was 300°C and that of the lower section 400°C . Collected particles were smooth spheres having a diameter of $\approx 33 \mu\text{m}$ as deduced by optical and SEM microscopy [Figs. 3(a) and (b)]. Any larger particles formed by fusion of two or three particles while still liquid (doublets, shown in the left side of Fig. 3(b), or triplets) were separated out by subsequent sieving. Dissolution of styrene beads in toluene required a few hours at room tempera-

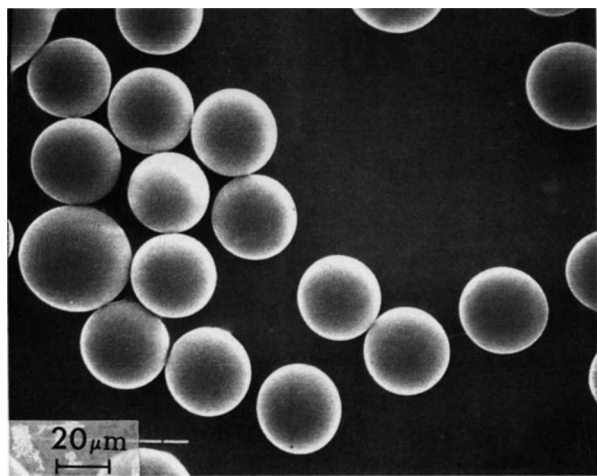
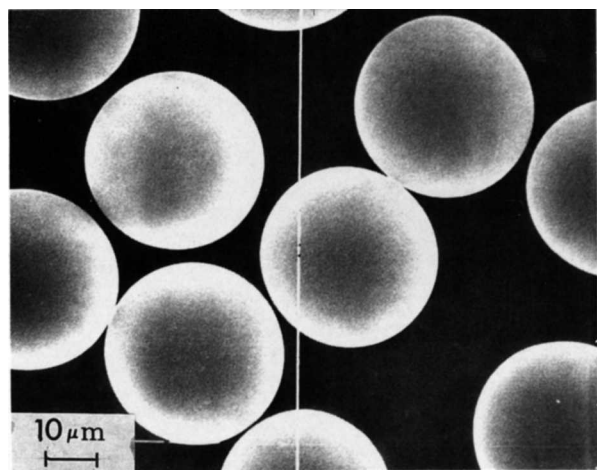


Figure 3 SEM micrographs of polystyrene particles. (a), $\times 1,000$; (b), $\times 500$.

ture and sonication prior to atomization was necessary to achieve uniform mixing. Insufficient mixing resulted in bubble formation. Furthermore, solutions thicker than 30 : 1 (toluene : polymer) were too viscous to handle properly and produce monodisperse particles. Extensive testing for monodispersivity of the droplets was done at the onset of each experiment using the test jet, described before. Optimum conditions for the reactor temperature and flow characteristics were determined by a combination of numerical modeling and experimental trials, with the following criteria in mind:

- To achieve vaporization of the solvent slowly enough to avoid formation of bubbles.
- To ensure that the residual polymer phase remains in the molten state to enable formation of spherical particles.
- To enable solidification of the particles, in the cooler bottom section of the reactor, before they reach the collection stage.

Overheating should be avoided since it might alter the chemical composition by pyrolyzing the polymer.

2. Production of polystyrene particles of $\approx 60 \mu\text{m}$ was achieved by generating an aerosol of partially polymerized styrene monomer. The monomer was mixed with benzoyl peroxide (2% by weight) and heated at $83\text{--}84^\circ\text{C}$ in a nitrogen atmosphere for 30 min. Subsequently, the semipolymerized precursor was dissolved in toluene at a ratio of 1 : 1 and passed through the thermal reactor in nitrogen atmosphere. Production was conducted at the same conditions as before with the exception of temperature, which was optimized for the current situation. The temperature profile in the reactor was controlled to prevent flash vaporization of the monomer. Thus, the top section of the reactor was set at a low temperature (240°C) to provide slow initial heat-up and the bottom section was hot enough (300°C) for the polymerization reactions to proceed to completion.

Poly(methyl methacrylate)

Batches of poly(methyl methacrylate) particles of 30–60 μm in diameter were produced by the above two techniques at similar conditions.

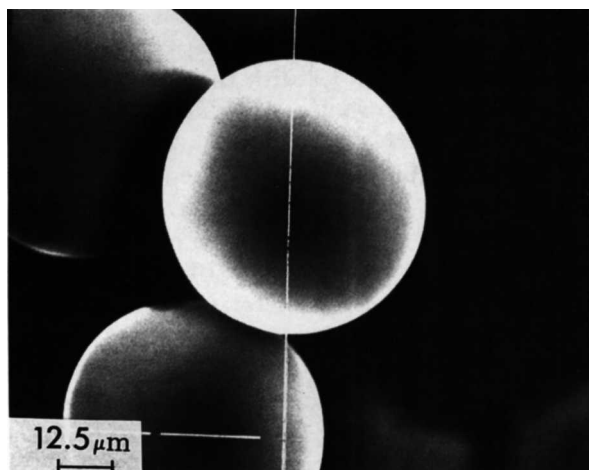


Figure 4 SEM micrograph of poly(methyl methacrylate) particles produced in the lab from the monomer precursor ($\times 800$).

1. Solutions of 2% poly(methyl methacrylate) in acetone were atomized by the aerosol generator in conditions similar to those used for the poly(styrene) particles.
2. Methyl methacrylate was prepolymerized in bulk using benzoyl peroxide (2% by weight) as initiator. The polymerization was carried out at 75°C for 15 min, resulting in a partially reacted, medium viscosity liquid. This was then dissolved in acetone at a ratio of 2 : 1 (acetone : polymer) and conducted to the aerosol generator. The polymerization was then completed in the thermal reactor, with wall temperatures of 260 and 290°C at the top and bottom sections, respectively. Solid particles, 45 μm in diameter, were collected, as shown Figure 4.

CHEMICAL CHARACTERIZATION OF PARTICLES

The particles were characterized for chemical composition by elemental analysis and for molecular weight by an osmometry technique (Galbraith Labs). Elemental analysis for carbon and hydrogen (C,H) was conducted on all particles produced as well as the commercial polymer precursors. Results are shown in Table I. The numbers in parentheses indicate the theoretically expected composition as calculated from the molecular formula of the polymer.

It can be seen from Table I that the C and H composition of the produced particles is very close to that of their polymer precursors and also to the theoretically expected compositions. This can be considered as an indication that no substantial pyrolysis of the particles has taken place throughout the thermal treatment of the polymers. The molecular weight of those particles that were produced from monomer polymerization is somewhat lower than that expected, based on the amount of the initiator and the fact that no solvent was present during prepolymerization. This is probably due to the fact that the inhibitor present in commercially available monomers was not removed prior to polymerization in these experiments.

NUMERICAL SIMULATION OF THE PARTICLE HEAT TREATMENT

To model the velocity and temperature environment in the thermal reactor, the FLUENT software package (Creare, 1989) was utilized. Numerical solutions for the gas phase were obtained by simultaneously solving the continuity, momentum, and energy equations. The program was used to study the effects of the reactor geometry, gas flow rates,

Table I Material Properties

Polymer Type	Carbon (wt %)	Hydrogen (wt %)	Mol. Weight
Poly(styrene) beads (commercially available)	91.66 (92.25)	8.00 (7.75)	—
Poly(styrene) particles (from dissolved polymer)	91.14 (92.25)	7.78 (7.75)	—
Poly(styrene) particles (from monomer precursors)	91.25 (92.25)	7.73 (7.75)	3,594
Poly(methyl methacrylate) (commercially available)	59.78 (59.99)	8.39 (8.05)	—
Poly(methyl methacrylate) (from monomer precursors)	60.04 (59.99)	8.29 (8.05)	6,430

and wall temperature on the velocity and temperature profiles. Furthermore, an additional feature of this program dealt with the behavior of liquid drops introduced in the gaseous environment. Then, the trajectory of the drops, the time required for solvent vaporization, the residence time of the solid particle, and the particle heat-up characteristics were estimated. Results so obtained were used to find the optimum reactor temperatures for droplets of the polymer-solvent mixtures investigated herein.

A brief description of the calculations with FLUENT is given in the following: A finite difference grid is set up that divides the domain of the problem into a number of computational cells. Boundary conditions are specified at the inlet and walls of the domain. The equations of continuity, the momentum, and energy for the gas phase are reduced to a set of simultaneous algebraic equations and an iterative scheme is used to find the solution of the system. When the solution of the gaseous phase converges sufficiently, the introduction of droplets takes place and the mass, heat, and momentum transfer between the gaseous phase and the droplets are calculated. The iterations continue until the solution converges.

Two different cases were modeled herein: (1) the production of poly(styrene) particles from 2.5 wt % dissolved polymer in toluene at reactor temperatures of 300 and 400°C (top and bottom sections) and (2) the production of polystyrene particles from the monomer precursor (50% by weight) dissolved in toluene. The reactor temperatures were 240 and 300°C this time. Various droplet sizes were modeled in the range of 30–144 μm in diameter.

Input to the model were the following:

- Geometry and the dimensions of the reactor—The overall length was 1.6 m and the inner diameter 0.1 m.
- Inlet velocities of the dispersion and the dilution gas streams—Their inlet flowrates were 1.0 and 2.5 lpm, respectively; the corresponding velocities were calculated to be 0.0055 and 7.46 m/s.
- Wall temperature of the reactor, estimated by measurements taken by four thermocouples attached to the outer surface of the reactor at different heights—The temperature between the thermocouples was assumed to change linearly. The maximum and minimum wall temperatures were set according to the experimental conditions used for the generation of the various particles.
- Flow type, which was here considered turbulent because of the vigorous mixing of the high-velocity dispersion jet with the slow-moving dilution gas—Turbulence was assumed despite a low Reynolds number, ($Re = 25$), calculated far away from the mixing zone (at midreactor height).
- Initial size of the droplets, as calculated from the formula¹³: $D_d = (6Q/\pi f)^{1/6}$, where D_d is the initial droplet diameter, Q is the volumetric flowrate of liquid forming the aerosol, and f is the imposed frequency. For the values of Q and f mentioned earlier, the initial droplet diameter was calculated to be 144 μm. The corresponding initial axial velocity of the droplets ($u = 4Q/\pi D_o^2$, where D_o is the diameter of the orifice) was calculated to be 6.06 m/s. Furthermore, to investigate the behavior of drops at various radial positions in the reactor initial radial velocity ranging from 0.1–0.5 m/s were input. The droplets consisted of a volatile solvent (toluene or acetone) that evaporated and diffused into the reactor gaseous phase and a solid content that heated but did not evaporate, simulating the polymer. It should be noted here that devolatilization of the polymer, if any, was not taken into account in the present study.
- Finally, the physical constants of the gaseous (nitrogen) and the droplet (predominantly solvent) phases were input as a function of temperature. Since the model assumes average

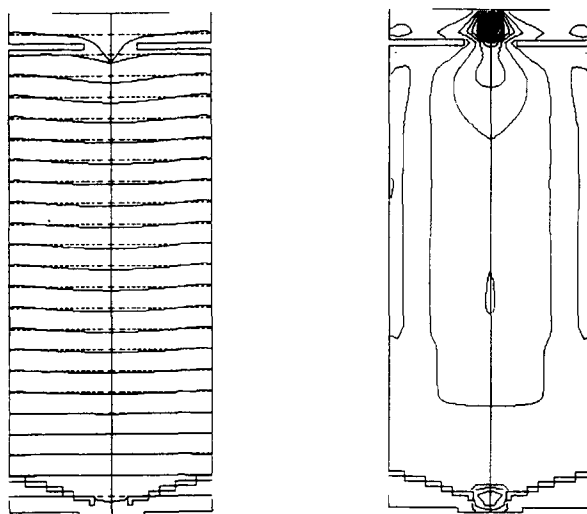


Figure 5 Results of numerical simulation for gas flow in the thermal reactor (a) axial velocity profiles and (b) axial velocity contours. Maximum wall temperatures were 300 (573 K) and 400°C (673 K) in the upper and lower stages, respectively.

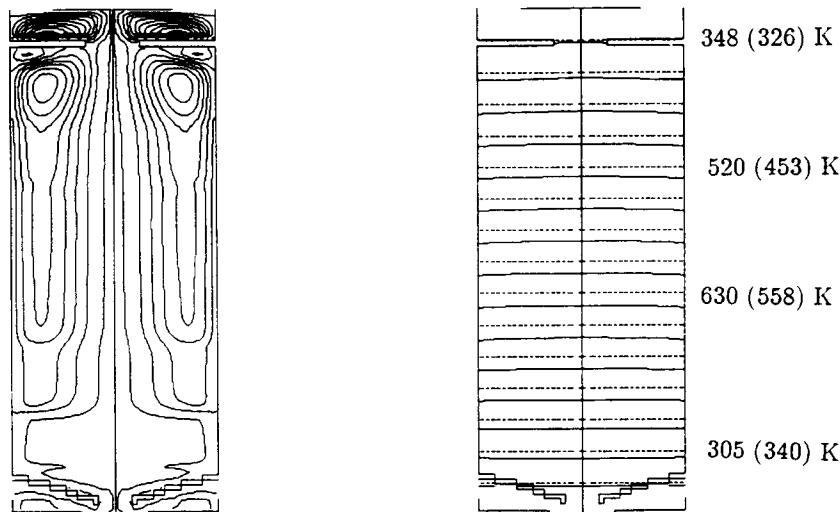


Figure 6 Results of numerical simulation for gas flow in the thermal reactor (a) flow streamlines and (b) temperature profiles. Wall temperatures and centerline temperatures (in parentheses) are shown. Maximum wall temperatures were 300 (573 K) and 400°C (673 K) in the upper and lower stages, respectively.

properties for the two constituents of the droplet, the solid particle diameter (after the vaporization stage) was overestimated because the density was biased toward that of the more abundant solvent. Corrections for the real polymer density had to be applied.

RESULTS OF THE NUMERICAL MODELING

The theoretically predicted thermal environment inside the reactor is shown in Figures 5 and 6 for case (1) above, where the maximum wall temperatures were 300 (573 K) and 400°C (673 K) for the upper and lower stages, respectively. The axial velocity profiles along the reactor are depicted in Figure 5(a). Both the dispersion and the concentric dilution streams are shown, with the former diffusing relatively fast in the slow-moving dilution gas stream. The presence of the orifice plate situated downstream of the jet inlet was found helpful in preventing buoyant gases from rising, along the walls, to the very top of the reactor. The presence of these hot gases in close proximity to the inlet of the droplets can cause rapid evaporation of the solvent and result in bubble formation, as mentioned before; moreover, as hot gases condense on the cooler surfaces of the observation window obstruct the view to the jet. In Figures 5(b) and 6(a), the contours of the axial velocities and the streamlines are shown. It can be observed that the presence of buoyancy highly disturbs the flow pattern and induces circu-

lation of gases near the walls of the reactor. Thus, in addition to the presence of the orifice plate it was determined that application of suction at the exhaust of the reactor was necessary to control the flow field in the reactor. The temperature profiles along the reactor are shown in Figure 6(b), where it can be seen that the center-line temperature of the inlet streams is an average of 50 K below the wall. Similar

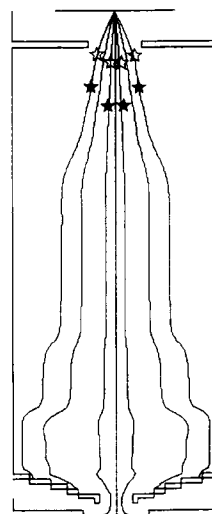


Figure 7 Results of numerical simulation for the droplet-particle phase showing tracks of equal size droplets (144 μm) having different initial radial velocities (0.1–0.5 m/s). Completion of solvent evaporation is denoted by (☆) for acetone and by (★) for toluene. Conditions are corresponding to Figures 5 and 6.

temperature and velocity profiles were obtained for other experimental conditions used in this study.

Droplet trajectories are shown in Figure 7, corresponding to the conditions of Figures 5 and 6. All droplets depicted in Figure 7 had the same initial size, 144 μm , but different radial velocities (0.1–0.5 m/s). The droplets experienced an initial heat-up

and evaporation period where the solvent diffused to the gaseous phase; the end of this period is marked with asterisks in Figure 7. Times for solvent vaporization were calculated to be ≈ 0.17 and 0.07 s (for toluene and acetone, respectively) [Figs. 8(a) and (b)]. It should be noted here that according to the model used the vaporization of most of the solvent

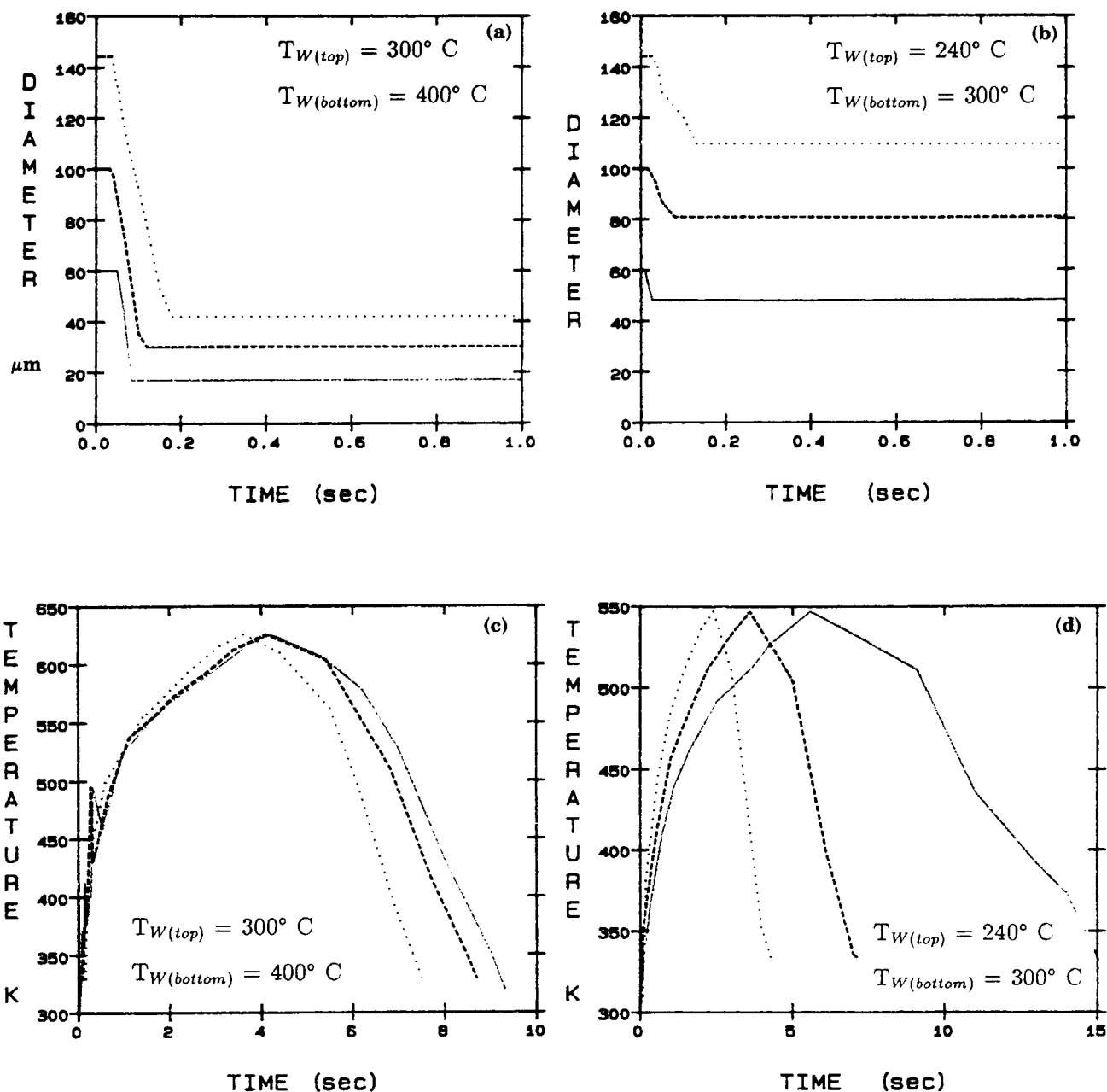


Figure 8 Results of numerical simulation depicting (a) and (b) droplet size for cases (1) and (2), (c) and (d) particle temperature for cases (1) and (2); all as functions of time for initial droplet sizes 60 (—), 100 (---), and 144 (· · · · ·) μm . The solvent was toluene. Corresponding wall temperatures are marked on the figures.

was completed before the boiling point of toluene or acetone were reached (383 and 330 K, respectively) and, hence, the process was diffusion controlled. Upon evaporation, the particles follow the trajectories depicted in Figure 7 and experience further heat-up till they reach the local gas temperature. Total residence times were calculated in the range of 7.5–14 s, depending on each particle's path. Therefore, to produce particles that experience the same residence time in the reactor and result in uniform properties the particles should flow in a rather narrow stream around the reactor centerline. Furthermore, narrow streams minimize the deposition of particles on the upper surfaces of the funnel, as shown at the bottom of Figure 7. Then, even if the above arguments indicate that narrow droplet streams are desired, a certain amount of dispersion is required to avoid droplet coagulation, thus a compromise should be determined experimentally. Moreover, the problem becomes more complicated since even small instabilities of the droplet stream can initiate a rapid succession of collisions and result in a polydisperse aerosol.¹³

Results obtained for case (2) above indicate shorter residence times, 4–6 s, almost half of those found in case (1). This is partially due to the bigger size of the dry particles (higher solid content) and to reduced buoyancy at the lower wall temperatures of this case.

To investigate the effect of size on the residence time of the particles, Figures 8(a) and (b) are included where calculations of the variation of droplet

diameter and temperature with time, respectively, are depicted for particles of diameters ranging between 60–144 μm but with the same radial velocities. The total residence times for those particles flowing around the centerline range between 9–7 s for case (1) and 4–14 s for case (2). It can be seen that the solvent evaporation takes a very small fraction of the total residence time (about 2%). The solidification and the completion of the polymerization requires about 80% of the residence time, while the rest is consumed in the cool-down of the particle.

Velocity profiles of the gas as it flows through the virtual impactor are shown in Figure 9(a). This particular impactor was designed to operate with a particle collection efficiency of 60% for particles having diameters bigger than 10 μm .¹⁴ In Figure 9(b), the trajectories of two particles of different sizes that flow through the reactor and pass through the impactor stage can be seen. The bigger particle, 42 μm in diameter after evaporation, is trapped in the collection stage while the smaller, 8 μm , exits the reactor following the gaseous phase. Thus, any fine particles that are formed by nucleation and condensation reactions in the gas phase escape the impactor following the exhaust stream.

SUMMARY

Spherical and monodisperse particles of poly(styrene) and poly(methyl methacrylate) in the size range of 30–60 μm were produced by an acous-

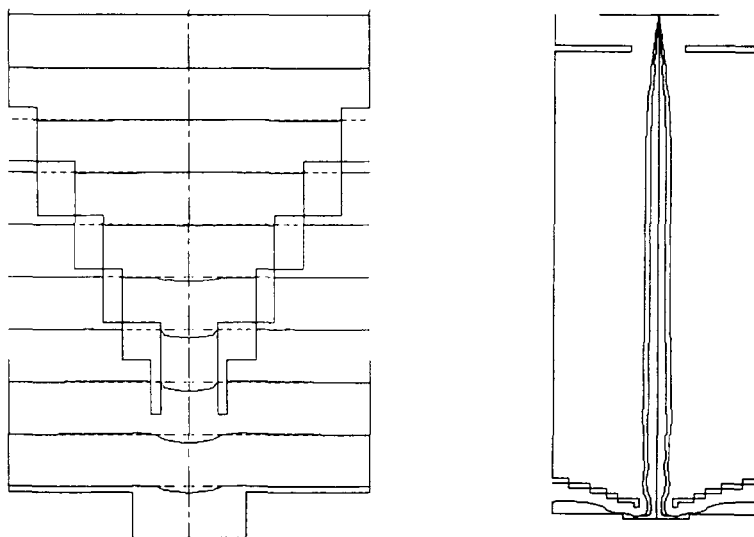


Figure 9 Results of numerical simulation showing (a) gas velocity profiles in the virtual impactor stage of the furnace and (b) particle tracks through the reactor for two droplet (dry particle) sizes: 144 (42) and 30 (8) μm .

tically excited aerosol generator. The generator formed a monodisperse spray from either mixtures of polymers and their solvents or monomers with initiator catalysts and solvents. As the spray passed through a thermal reactor in nitrogen atmosphere, the solvent evaporated and solid, spherical polymer particles were formed. The chemical composition of the particles was found to be close to that deduced from the chemical formula. The above technique can be used for the production of a variety of monodisperse particles of (1) organic or inorganic solids that can dissolve and result in solutions of relatively low viscosity or (2) polymers from their monomer precursors whose polymerization can be conducted in bulk.

Thermal treatment of the droplets was studied theoretically using numerical techniques. Results concerning the velocities and temperatures of both gas and particles, as well as the solvent evaporation and particle residence times, were obtained.

This research was supported by the NSF Initiation Grant CTS-8908652. The authors gratefully acknowledge assistance from Marina Belopolski in the experiments and Jonathan Doughty in the construction of the thermal reactor.

REFERENCES

1. D. B. Sicilia, *Invent. Tech.*, Spring/Summer, p. 45, (1990).
2. L. B. Adams, E. A. Boucher, R. N. Cooper, and D. H. Everett, Third International Conference on Industrial Carbon and Graphite, Soc. Chem. Ind., London, 1970, p. 478.
3. D. H. Everett and F. Rojas, *Chem. Soc., Faraday Trans. 1*, **84**(5), 1455 (1988).
4. P. Pendleton, B. Vincent, and M. L. Hair, *J. Coll. Interf. Sci.*, **80**, 512 (1981).
5. G. J. Howard and S. Knutton, *J. Appl. Polym. Sci.*, **19**, 683 (1975).
6. D. P. Bhanti, S. K. Dua, P. Kotrappa, and N. S. Pimpal, *J. Aerosol Sci.*, **9**, 261 (1978).
7. R. E. Partch, K. Nakamura, K. J. Wolfe, and E. Matijević, *J. Coll. Interf. Sci.*, **105**, 560 (1985).
8. R. E. Partch, E. Matijević, A. W. Hodgson, and B. E. Aiken, *J. Polym. Sci., Polym. Chem. Ed.*, **21**, 961 (1983).
9. K. Nakamura, R. E. Partch, and E. Matijević, *J. Coll. Interf. Sci.*, **99**, 118 (1984).
10. S. Gangolli, R. E. Partch, and J. Matijević, *Coll. Surfaces*, **41**, 339 (1989).
11. Y. A. Levendis and R. C. Flagan, *Comb. Sci. Tech.*, **53**, 117 (1987).
12. Y. A. Levendis and R. C. Flagan, *Carbon*, **27**, 265 (1989).
13. R. N. Berglund and B. Y. H. Liu, *Environ. Sci. Tech.*, **7**, 147 (1973).
14. J. A. Mulholland, G. X. Yue, and A. F. Sarofim, manuscript in preparation, 1990.
15. P. Biswas, PhD thesis, Caltech, 1985.

Received December 21, 1990

Accepted January 31, 1991